Separation Science and Technology
Publication details, including instructions for authors and subscription information:
http://www.informaworld.com/smpp/title~content=t713708471

Flux and Fouling in the Crossflow Ceramic Membrane Microfiltration of Polymer Colloids

Jiří Cakl[a]; Petr Mikulášek[a]
[a] DEPARTMENT OF CHEMICAL ENGINEERING, UNIVERSITY OF PARDUBICE, PARDUBICE, CZECH REPUBLIC

To cite this Article Cakl, Jiří and Mikulášek, Petr(1995) 'Flux and Fouling in the Crossflow Ceramic Membrane Microfiltration of Polymer Colloids', Separation Science and Technology, 30: 19, 3663 — 3680
To link to this Article: DOI: 10.1080/01496399508014151
URL: http://dx.doi.org/10.1080/01496399508014151

SEPARATION SCIENCE AND TECHNOLOGY, **30**(19), pp. 3663–3680, 1995

Flux and Fouling in the Crossflow Ceramic Membrane Microfiltration of Polymer Colloids

JIŘÍ CAKL* and PETR MIKULÁŠEK
DEPARTMENT OF CHEMICAL ENGINEERING
UNIVERSITY OF PARDUBICE
NÁM. ČS. LEGIÍ 565, 532 10 PARDUBICE, CZECH REPUBLIC

ABSTRACT

The results of an experimental study of ceramic membrane microfiltration of synthetic polymer colloids differing greatly in average particle size and distribution broadness are presented. The effects of the polymer nature, pressure difference, feed velocity, and particle to membrane pore diameter ratio on the permeate flux and membrane fouling are discussed. Attempts have also been made to explain the results in terms of simple models of the operative mechanisms.

INTRODUCTION

Polymer colloids (latexes) are colloidal dispersions of submicron polymer particles in an aqueous medium. The system usually contains a number of ingredients. Some ingredients are added in the original polymerization recipe such as initiator and emulsifier molecules; other are generated during the course of the polymerization process such as oligomers and functional surface end-groups on the particles; while surface-active compounds, water-soluble polymers, thickening agents, pigments, and biocides are added as postpolymerization additives.

The dispersion particles are generally spherical, and the particle size may vary from several hundred angstroms to several microns. The particle size distribution may be very broad or very narrow and can be controlled to a high degree by polymerization conditions. Polymer colloids generally

* To whom correspondence should be addressed.

are considered to be metastable systems. The chief forces that affect stability are: a repulsive force, which results from the interaction of similarly charged particle surfaces; entropic repulsive forces, which are generated by steric hindrance of solvation of the adsorbed layers; and attractive forces of the London–van der Waals dispersion type. The parameters that can perturb these forces are electrolyte addition, mechanical collisions between particles (i.e., in a shear field), thermal effects, and organic solvent addition. In most latex applications, including membrane separation, coagulation can be undesirable, and therefore stability under potentially perturbing conditions is a goal.

The concentration of in-process polymer colloids streams was one of the early applications suggested for membrane separation, namely ultrafiltration (1). For example, in the case of poly(vinyl chloride) latex, the dry solids content may be increased from 30 to 65 wt%. The second application is the concentration of dispersed colloid particles from 0.1 to 25 wt% or more as a pollution control technique and frequently as a means of recovering valuable dilute polymer for reformulation (i.e., from tank washing solutions). Poly(styrene–butadiene) and poly(vinyl acetate) latexes are prime examples. The third application is the purification of polymer dispersion in a dilution mode (diafiltration), thereby eliminating oligomers, catalyst residue, and salts.

The large amount of work dealing with this subject is mostly related to the use of organic ultrafiltration membranes, although there are at least three main advantages in using ceramic microfiltration membranes: 1) low membrane resistance, 2) the possibility to treat very viscous feeds (high solids contents), and 3) the effective antifouling and cleaning procedures available for microfiltration ceramic membranes enable higher steady-state flux to be maintained for long periods. In general, there are many similarities between microfiltration carried out in the crossflow mode and ultrafiltration. The hydrodynamic pattern is similar, the hardware is very similar, and the problems with flux decline are nearly the same. The membranes are different, although ultrafiltration may be carried out with microporous membranes (and secondary membranes are formed on top of them). Nevertheless, there are some potential drawbacks in using microfiltration for treatment of polymer colloids which should be studied, i.e., stronger internal pore fouling tendency and the possibility of lower selectivity for the recovery of a specific product.

The advantages of crossflow microfiltration are enhanced by the general observation that fluxes obtained for submicron colloids are usually significantly higher than those predicted from theories developed for macrosolute ultrafiltration (2–4). Attempts to explain this flux anomaly frequently invoke a liquid-mechanical enhancement of particle transport out of the

polarized layer. The models of shear-induced particle diffusivity (2, 5) and lateral migration (2, 6, 7) are the most popular. It has also been shown by McDonogh et al. (8) that the factors which control concentration polarization in crossflow membrane separation may be charge dependent. The formation of fouling layers of dispersed materials on the membrane surface (filter cake) can also be important in the microfiltration of polymer colloids. The specific resistance of such cakes is a function of the particle shape and diameter as well as the charge properties of the particles. In addition, the membranes cannot be understood simply as sieves; therefore, the electrochemical properties of the membrane surface and dispersed particles can have a significant influence on the nature and magnitude of the interactions between the membrane and the dispersion being processed.

In the present study ceramic membrane microfiltration of polymer colloids has been studied in some detail. The effects of the particle nature, pressure difference, feed velocity, and the colloid particle to membrane pore size ratio on both the permeate flux and probable membrane fouling mechanisms are discussed. Attempts have also been made to explain the process behavior in terms of simple models of the operative mechanisms.

EXPERIMENTAL

The membranes used were alumina-based, tubular, internal-pressure-type ceramic microfiltration membranes supplied by Terronic (Hradec Králové, Czech Republic). They were configured as single cylindrical tubes 0.1 m long, with an inside diameter of 6 mm and an outside diameter of 10 mm, consisting of a thin α-alumina layer on top of a support. For the measurements two types of membranes were used with nominal pore sizes of 0.1 μm (Membrane 1) and 0.2 μm (Membrane 2). The membrane pore size distribution was determined using the modified bubble point test (9). The distributions obtained are shown in Fig. 1. Membrane characterization by scanning electron microscopy showed the thickness of the active layer to be about 20 μm. The specific hydraulic resistances of the membranes were determined during permeation of ultrapure water and gave the values $R_M = 9.1 \times 10^{11}$ m^{-1} (Membrane 1) and 6.04×10^{11} m^{-1} (Membrane 2).

Two kinds of feed were used in the crossflow apparatus: commercial dispersions of poly(vinyl chloride) (PVC) and acrylic copolymer (AC) latexes. These were suspended in deionized water. Concentration of the polymer colloid particles was 1% (w/w) solids. Characterization of colloids with a particle sizer BI-90 (Brookhaven Instruments Corporation) and SediGraph 5100 (Micromeritics), respectively, showed each feed to be

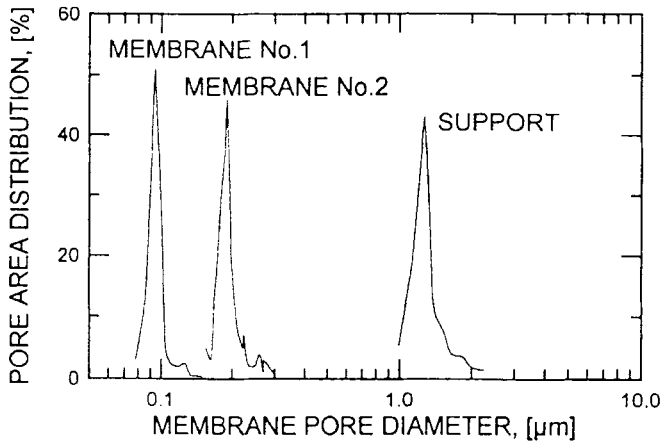

FIG. 1 Pore size distribution of the active layers and porous support of the alumina microfiltration membranes used.

polydisperse (see Fig. 2). Electron microscopy showed the particles to be near perfect spheres in the case of the acrylic latex; multiple agglomerates were detected in the PVC latex. The specific resistances of the filtration cake created by the colloid particles used were evaluated from dead-end filtration experiments. The solid volume fraction in the cake layer formed by AC-latex particles was calculated from the specific cake resistance by application of the Kozeny–Carman fixed bed flow equation (10). In the

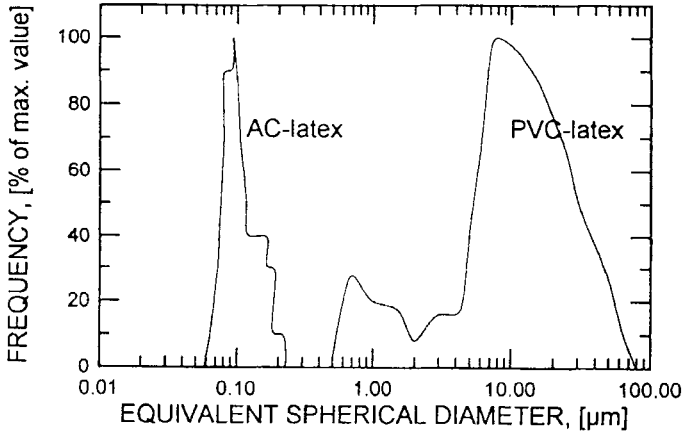

FIG. 2 Particle size distribution of the feeds used.

TABLE 1
Selected Properties of the Test Dispersions

Trademark	Composition	Particle density ($kg \cdot m^{-3}$)	Solid volume fraction (—)		Specific cake resistance per unit thickness (m^{-2})
			In the feed	In the cake	
Sokrat 6492[a]	Acrylic copolymer (AC)	1060	9.43×10^{-3}	0.590	1.87×10^{17}
E-632[b]	Poly(vinyl chloride) (PVC)	1432	6.98×10^{-3}	0.439	7.48×10^{14}

[a] Manufactured by Chemické závody Sokolov, Czech Republic.
[b] Manufactured by CHZ Nováky, Slovak Republic.

case of the much more permeable PVC-latex filtration cake each piece of membrane was dried and weighed before the filtration run and its weight was determined again after filtration and drying. Together with the measured cake thickness, this gave information about the total amount of deposited material and solid volume fraction in the cake. The results obtained are summarized together with other characteristics in Table 1.

The microfiltration studies were carried out in a crossflow filtration unit equipped with a membrane module formed from a membrane placed in an acrylic casing. Latex dispersions were circulated through the module by a piston pump with the feed flowing parallel to the membrane surface and perpendicular to the permeate. The unit allowed studies in which transmembrane pressure and crossflow velocity were varied independently. A new membrane was used in each experiment, and before the run the pure water flux was measured with deionized water. A dispersion of polymer colloid was then introduced to the unit, the pump was turned on, and the operating pressure was adjusted by the regulation system. The flux through the membrane was measured by collecting the permeate in a graduated cylinder and timing the collection period. Both permeate and retentate were recycled to the reservoir to maintain a relatively constant latex concentration and ionic environment. Every experiment was carried out until the flux became virtually constant. Duplicate microfiltration experiments for selected conditions showed good reproducibility of the data measured.

RESULTS AND DISCUSSION

The experimental data showed a trend with higher fluxes for the PVC latex compared with the acrylic copolymer latex. The steady-state flux

which was usually reached was lower than the pure water flux; it ranged from 5 to 70% of the pure water flux.

Analysis of the permeate composition showed complete rejection of the colloid particles in the retentate in the majority of cases. This is not surprising considering that PVC latex particles are large compared to the membrane pore size. If size exclusion is considered as a separation mechanism for AC latex, colloid size is not sufficient to explain the high retention obtained (compare Figs. 1 and 2). This could probably be attributed to electrostatic repulsion occurring between the membrane and the colloids since both are negatively charged. Moreover, the formation of a dynamic membrane on the membrane surface can also be important. It seems that a deposit made up of the feed particles has nearly 100% retention for this type of particle.

Initial Flux Decline

The time dependence of the flux decrease at different applied feed velocities is shown in Fig. 3 for PVC latex and in Fig. 4 for AC latex at the feed concentrations of 1 wt% solids and a transmembrane pressure difference of 100 kPa. Besides the fact that high levels of permeate flux are achievable, thus making the process economically attractive, the most noticeable feature in Figs. 3 and 4 is the very significant dependence of the flux decline on the feed flow and the type of latex used, as well as on the particle to pore diameter ratio.

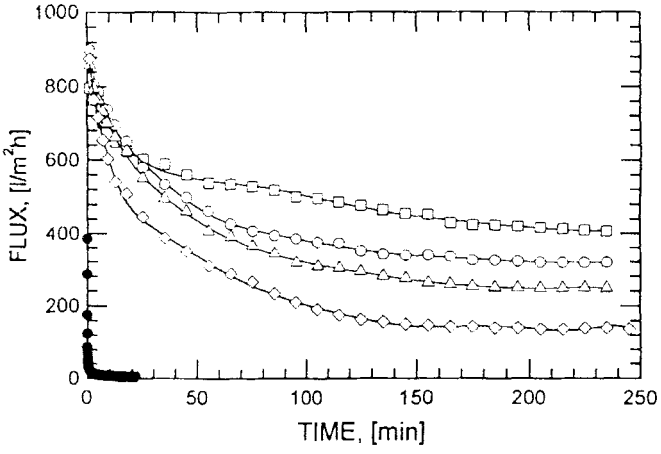

FIG. 3 Variation of the flux with time during microfiltration of PVC latex dispersion through Membrane 2. Transmembrane pressure difference: 100 kPa; feed velocity: (◇) 0.08 m/s, (△) 0.94 m/s, (○) 2.21 m/s, (□) 3 m/s, (●) dead-end.

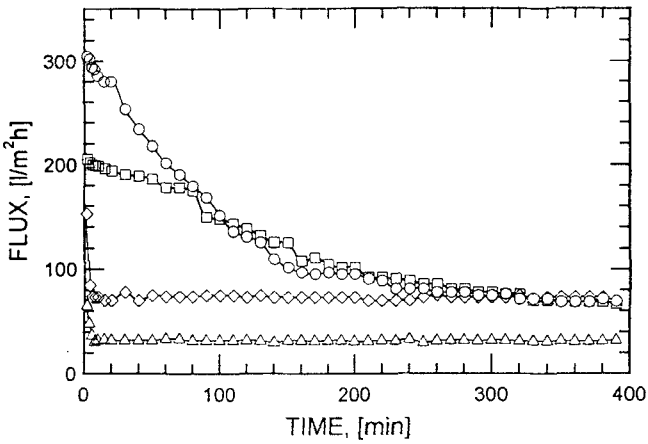

FIG. 4 Variation of the flux with time during microfiltration of AC latex dispersion through Membrane 1. Transmembrane pressure difference: 100 kPa; feed velocity: (△) 0.44 m/s, (◇) 0.94 m/s, (○) 1.82 m/s, (□) 2.88 m/s.

Chronologically it is possible to identify two separate phases of the initial flux decline. First, reversible concentration polarization builds up within the first minute. Then flux continues to decline for up to several hours due to polymer colloid deposition on the front surface of the membrane or within the membrane pores. To show which of the mechanisms may be dominant in the second phase of the process, we have analyzed experimental microfiltration data in terms of the transient flux filtration models. These are mostly modified blocking and cake-based models originally developed to describe the fouling process for dead-end microfiltration (11, 12). Probably due to the simplicity of their mathematical expression, some authors [e.g., Refs. 13–15) have been inclined to analyze the experimental results of crossflow filtration processes by means of these models, too. The relevant model equations can be written in the form:

Cake filtration:

$$\frac{1}{J} = \frac{1}{J_0} + K_C V \tag{1}$$

(i.e., $1/J$ versus V should be linear)

Complete blocking filtration:

$$J = J_0 - K_B V \tag{2}$$

(i.e., J versus V should be linear)

Intermediate blocking filtration:

$$\frac{1}{J} = \frac{1}{J_0} + K_I t \tag{3}$$

(i.e., $1/J$ versus t should be linear)

Standard blocking filtration:

$$\sqrt{\frac{J}{J_0}} = 1 - \frac{K_S V}{2} \tag{4}$$

(i.e., $\sqrt{J/J_0}$ versus V should be linear)

Here, J is the permeate flux, J_0 is the initial (pure water) flux, V is the total permeate volume collected until time t, and K_C, K_B, K_I, and K_S are the cake and blocking filtration constants, respectively.

By plotting filtration data in these various forms, the dominant filtration mechanism can be identified. An example of the cake and intermediate blocking law analysis is given in Fig. 5 for AC latex and in Fig. 6 for PVC latex. For the sake of clarity the steady-state values are omitted in Fig. 6. For AC latex the intermediate blocking law (empty symbols) gives the best fit for all experimental runs, with a coefficient of linear regression

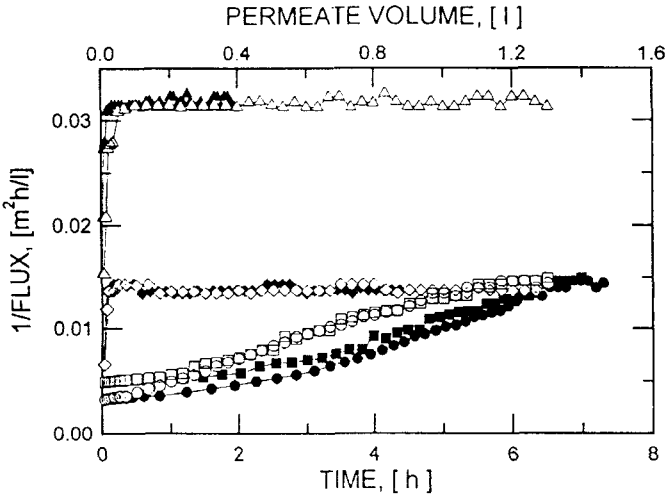

FIG. 5 Estimation of the fouling mechanism during the microfiltration of AC latex through Membrane 1. Transmembrane pressure difference: 100 kPa; feed velocity: (△) 0.44 m/s, (◇) 0.94 m/s, (○) 1.82 m/s, (□) 2.88 m/s. The filled symbols are for the permeate volume dependence, while the empty symbols are for time dependence.

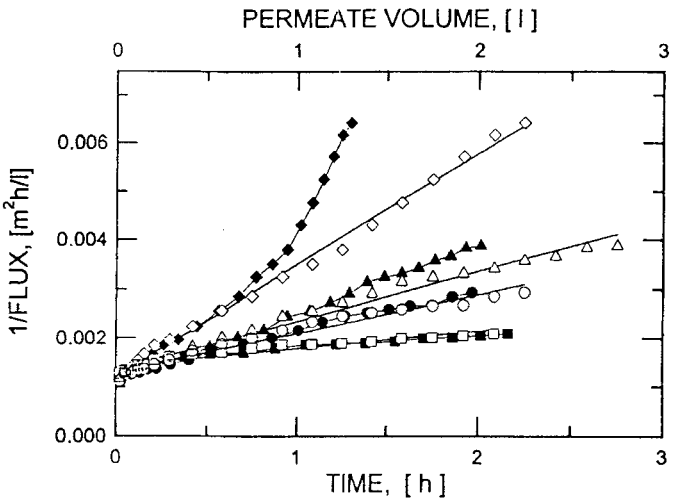

FIG. 6 Estimation of the fouling mechanism during the microfiltration of PVC latex through Membrane 2. Transmembrane pressure difference: 100 kPa; feed velocity: (◇) 0.08 m/s, (△) 0.94 m/s, (○) 2.21 m/s, (□) 3 m/s. The filled symbols are for the permeate volume dependence, while the empty symbols are for time dependence.

higher than 0.96. The cake filtration law (filled symbols) also gives linear dependence in the case of PVC latex for all runs except for the one with the lowest feed velocity. The opposite trend is evident from Fig. 5 in which the assumed cake filtration of AC latex is characterized by a nonlinear dependence of variable (1/flux) vs permeate volume mainly for higher velocities.

We can conclude that the cake build up prevails if the particles are larger than the pores (PVC latex). The observed apparent pore blocking for the feed velocity 0.08 $m \cdot s^{-1}$ can be a result of continuous enrichment of the cake layer with the fine particle fraction. This idea has also been confirmed by a higher solid volume fraction in the filter cake in comparison with the dead-end filtration run. From the point of view of filtration theory, this behavior can be considered similar to a cake pore blocking phenomenon. Similar results were obtained by Reismeier et al. (16). They suggested that the increased resistance arose because, particularly at lower permeation rates, larger particles were preferentially removed from the membrane surface, resulting in a more tightly packed cake of smaller particles.

Another behavior occurs if the active layer pore size is very close to the diameter of the particles filtered (as in the case of AC latex). If the

particles are sufficiently flexible, they can enter the pore and remain inside, probably due to some interaction with the membrane material. When the feed velocity is lower than 1 $m \cdot s^{-1}$, the period of pore filling may be short. The pores may only be slightly entered by particles which begin instantly to bridge over the pore and form a very thin filter cake. This deposit can be taken as a secondary membrane which protects the microfiltration membrane against plugging by particles and therefore contributes to a higher and more stable flux. Depending on the shear forces developed by the feed flow, the cake thickness is decreased, and in the limiting case the cake cannot be further created under the given hydrodynamic conditions. Thus the membrane surface is open for smaller particles contained in the polydisperse feed to enter the membrane structure and block large pores. This also can be the explanation of the qualitatively different flux decline presented in Fig. 4 for the higher feed velocities.

Steady-State Flux

As microfiltration proceeds, the filtration rate eventually reaches a limiting or pseudo-steady-state value. The limiting value is approached when further growth of the filter cake is hindered by the applied axial fluid shear upon the system. In a pseudo-steady-state period the flux declines slowly, probably due to further internal deposition of particles into the membrane or to compaction of the fouling layer. By analogy to the standard Darcy filtration model, steady-state flux J_{ST} can be considered to be controlled by several resistances in series:

$$J_{ST} = \frac{\Delta P}{\mu(R_M + R_{PB} + R_{PA} + R_{FD} + R_{BL})} \tag{5}$$

where ΔP is the transmembrane pressure, μ is the permeate viscosity, and the R_i's are respectively the resistance of the membrane, the resistances due to membrane pore blocking and adsorption onto pores, as well as the resistances of the fouling deposit and boundary layer.

Effect of Transmembrane Pressure Difference

In Fig. 7 the steady-state flux data are plotted versus the transmembrane pressure difference for the systems investigated. If the particles were bigger then the pores, i.e., in the systems with PVC latex, it was found that the flux increases linearly with pressure difference at low values up to a critical pressure difference, then the rate of increase decreases, and finally the flux becomes nearly independent of pressure difference at high values. These findings support the well-known fact that both the membrane and the cake resistance are dominant for low pressure differences, whereas the boundary layer resistance is dominant for high pressure differences.

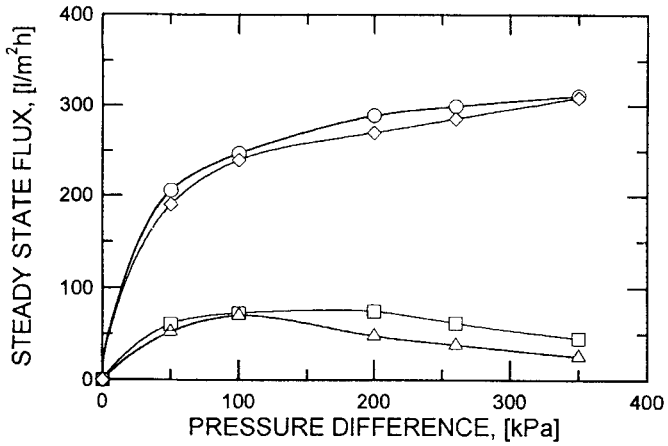

FIG. 7 Variation of the flux with transmembrane pressure difference for feed velocity 0.95 m/s: (□) microfiltration of AC latex through Membrane 1, (△) microfiltration of AC latex through Membrane 2, (◇) microfiltration of PVC latex through Membrane 1, (○) microfiltration of PVC latex through Membrane 2.

The pressure dependencies of steady-state flux of AC latex dispersions are also shown in Fig. 7. In comparison with the PVC latex results, there is an optimum pressure below which the driving force is too low and above which increased fouling causes a large reduction in flux. This could be attributed to the formation of a filtration cake with higher resistance once the deposited colloid particles undergo compaction under higher transmembrane pressures. However, as can be seen from Fig. 7, the flux curve shifts to higher fluxes with Membrane 1 and the optimum pressure decreases with increasing membrane pore size. Thus a more likely hypothesis is that the initial internal membrane fouling is both feed velocity and pressure dependent, and its degree is affected by the membrane pore size. We conclude that both the internal fouled membrane and the secondary membrane are dominant resistances.

Effect of Feed Velocity

The steady-state flux data are plotted versus feed velocity on a log-log scale in Fig. 8. A nearly linear dependence was found for PVC latex, which confirms a power law relationship between flux and feed velocity. The regression line has the slope of one-third predicted by the concentration polarization model with Brownian diffusion. On the other hand, as the ratio of membrane pore size to particle size increases, at least with

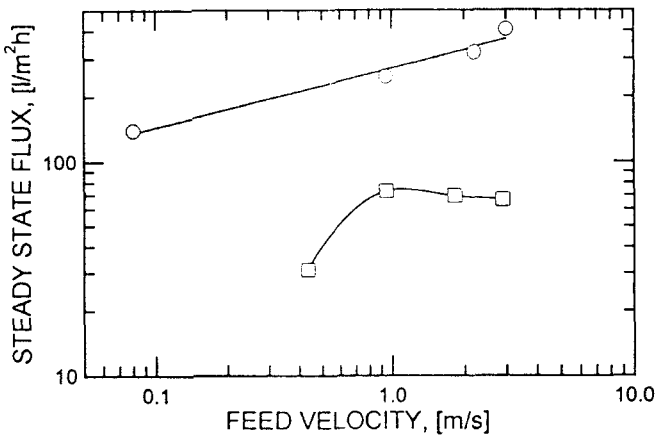

FIG. 8 Variation of the flux with feed velocity for transmembrane pressure 100 kPa: (○) microfiltration of PVC latex through Membrane 2, (□) microfiltration of AC latex through Membrane 1.

the AC polymer colloids used, the crossflow velocity has a limited effect. Bearing in mind the conclusions reached concerning initial flux decline with particles whose dimensions lie within the pore size distribution of the membrane, increasing crossflow velocity may improve the cake (secondary membrane) removal to such an extent that the membrane fouls internally.

Effect of Membrane Rinsing

To evaluate the irreversible membrane fouling, we have also considered the rinsing behavior of ceramic microfiltration membranes that had been fouled with the polymer colloids used. In experimental terms, irreversible membrane fouling represents the decrease in flux (compared with the original pure water flux) observed when the feed stream is replaced by pure water, supposedly leaving the irreversible fouling deposit intact. The flux increased quickly with rinsing, then flattened out and appeared to asymptotically approach a final value after 30 minutes.

If the irreversible fouling tendencies of the membranes are compared, Membrane 1 shows a marginally lower fouling than Membrane 2, particularly at higher pressures and velocities. However, these trends are overwhelmed by the effect of polymer colloid type. The value of rinsing flux reached up to 82% of the pure water flux, indicating low irreversible foul-

ing for PVC latex. This ease of removal of the PVC latex deposits could be attributed to their looser packing as a result of multiple agglomerates detected in the feed. In contrast with these results, the rinsing data for AC latex showed higher flux reduction, giving values in the range from 5 to 26% of the original pure water flux. Increasing the feed velocity (operating conditions for both the microfiltration and rinsing were kept the same) decreased the recovery of flux during rinsing, suggesting greater fouling. When the feed velocity was lower than 1 $m \cdot s^{-1}$, i.e., for the secondary membrane control regime, the flux after rinsing increased markedly, but not to the same extent as in the case of PVC latex. These findings suggest that the large decrease in hydraulic permeability in the experiments must be caused by a hydraulic resistance in the cake deposit (secondary membrane) with an extra resistance caused by internal pore fouling. Since these water permeability measurements only give "black box" type information, a comparison with the results for initial flux decline analysis is necessary in order to discriminate the contribution of the fouling mechanisms.

Comparison with Theoretical Predictions

Assuming boundary layer control in the crossflow microfiltration of the polymer colloids used, the estimates of steady-state flux were calculated from the film theory using both Stokes–Einstein diffusion (2) and shear-induced diffusion (5). For particles of the size range studied, nondiffusive transport can also be dominant. Thus the theoretical predictions given by the model of lateral migration (6, 7) were determined. In contrast to the polydisperse systems used in our experiments, the theoretical models were derived for idealized dispersions of equisized spheres. Therefore the models were examined with particular attention being paid to particle size effects. The steady-state fluxes predicted by the models have been plotted versus particle diameter in Fig. 9 for AC latex and in Fig. 10 for PVC latex. The decrease in flux with increasing particle diameter is predicted using Stokes–Einstein diffusion, whereas increasing flux is obtained for shear-induced diffusivity and lateral migration. As shown in Fig. 9, the transition from ultrafiltration-type behavior (steady-state flux vs decreasing particle diameter) to microfiltration-type behavior (steady-state flux vs increasing particle diameter) should occur at a particle diameter of about 0.35 μm for the system with AC latex. This value is outside the size distribution of the polymer colloid studied (Fig. 2). Therefore, according to the models used, the Stokes–Einstein diffusion should prevail. If we assume that the behavior is dominated by the smallest particles present in the feed, the agreement of the experimental steady-state flux (73.2 $L/m^2 \cdot h$)

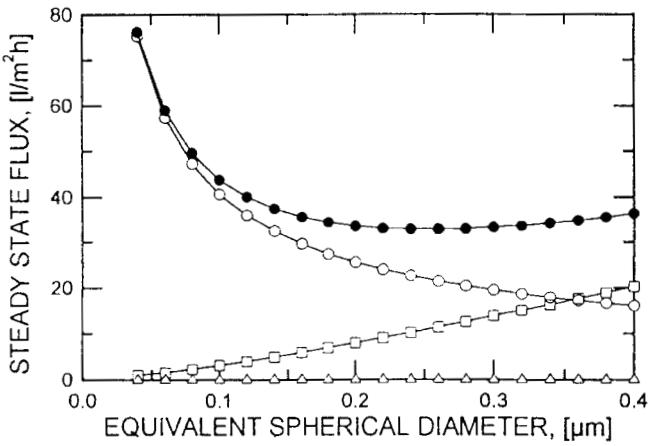

FIG. 9 Predicted variation of the flux with feed particle diameter for microfiltration of AC latex through Membrane 1 at feed velocity 0.94 m/s (Re = 5640, γ = 1254 s^{-1}): (○) Stokes–Einstein diffusion-based model, (□) shear-induced diffusion model, (△) lateral migration model, (●) added diffusion coefficients.

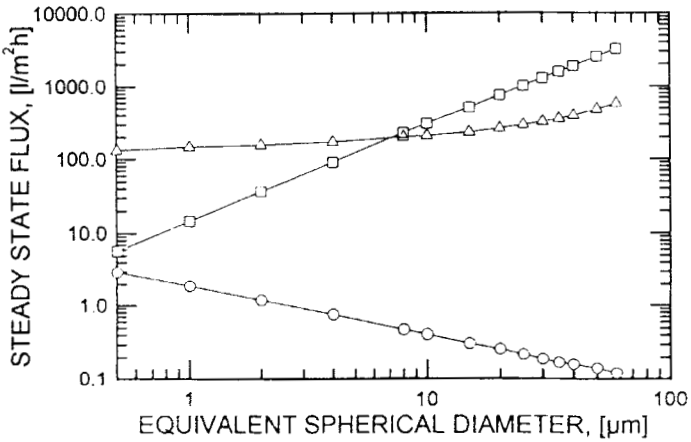

FIG. 10 Predicted variation of the flux with feed particle diameter for microfiltration of PVC latex through Membrane 2 at feed velocity 0.94 m/s (Re = 5640, γ = 1254 s^{-1}): (○) Stokes–Einstein diffusion-based model, (□) shear-induced diffusion model, (△) lateral migration model.

with predictions is apparently satisfactory. In contrast to the Stokes–Einstein diffusion model, the shear-induced diffusion model gives several times lower values for the steady-state flux. The inertial lift theory in this case underpredicts the steady-state fluxes by three orders of magnitude. There is probably an intermediate parameter range for which Stokes–Einstein and shear-induced diffusion could be considered simultaneously by adding the diffusion coefficients. In this case the predicted steady-state flux fits the experimental data better. However, in the present experiments with AC latex both the pore blocking R_{PB} and fouling deposit R_{FD} resistances are dominant. Only if the diffusive transport were dominant could the greater variation in R_{BL} than in R_{PB} or R_{FD} be accounted for.

A possible explanation for these results may lie in recent works (8, 17) on the effects of charge on the filtration of colloid systems. It was shown that electrostatic repulsion could have a significant effect on backtransport of particles. This electrokinetic enhancement was shown to increase with increasing zeta-potential of the colloids (calculated from electrophoretic mobility). However, at present it is difficult to apply a quantitative test of this hypothesis to real polydisperse systems. At the most fundamental level, conversion of electrophoretic mobility data to zeta-potentials is complex for polydisperse systems, especially if the colloid particles have a rough or hairy surface. The classical electrokinetic theory due to Smoluchowski and the even more elaborate treatment of O'Brien and White are invalid in this situation (18).

The system with PVC latex was chosen as an alternative to the AC latex, where the larger particles had a higher steady-state permeate flux (310.5 $L/m^2 \cdot h$). The low values of the relative system resistance (the ratio of the cake and membrane resistance) indicate that both the cake and membrane resistances were important in most of the experiments. Also, it has been shown that the boundary layer resistance is dominant for high pressure differences.

The dependence of the limiting steady-state flux versus particle diameter is shown in Fig. 10. When it is compared to Fig. 9 for the AC latex, two features are noteworthy. First, the Stokes–Einstein diffusion-based model underpredicts the limiting steady-state fluxes by several orders of magnitude. In contrast, the shear-induced diffusion and lateral migration models gave predictions of the right order of magnitude. Second, the predicted limiting steady-state flux is strongly particle diameter dependent. This phenomenon is not as pronounced in the case of the lateral migration model. Nevertheless, it seems that the polydisperse microfiltration feed used cannot be easily characterized by a simple average particle diameter for the purpose of these model calculations.

CONCLUSIONS

The results presented demonstrate that crossflow ceramic microfiltration membranes are useful for the removal or recuperation of poly(vinyl chloride) and acrylic polymer colloid dispersions from wastewater or process streams. The prime objective of process optimization is the minimization of fouling since it is the fouling layer and membrane pore blocking that control the permeate flux. It was shown that by carefully analyzing such operating parameters as the transmembrane pressure difference, crossflow velocity, and water-rinsing behavior, it may be possible to separate the various transport and fouling resistances which are extremely valuable for process optimization.

The experimental results indicate that both the particle size and electrostatic repulsion have a significant effect on the initial flux decline as well as the limiting flux, particularly if the membrane pore size is very close to the diameter of particles being filtered. The increase in the pressure difference as well as in the feed crossflow velocity does not always result in increased flux. It was shown that an adequate secondary membrane can protect the support microfiltration membrane against plugging by particles, and it therefore contributes to a higher and more stable flux.

Attempts have also been made to explain the process behavior in terms of simple models of the operative mechanisms. The models were examined with particular attention to particle size effects. It was shown that the flux behavior may not be explained simply in terms of conventional descriptions of lateral migration, Stokes–Einstein diffusion, and shear-induced diffusion. Further understanding will require experiments with real dispersions having broad size distributions and particles with well-defined electrokinetic properties.

ACKNOWLEDGEMENT

This work was financially supported by the Grant Agency of Czech Republic, Grant Project 104/93/2306.

NOTATION

J	permeate flux ($m \cdot s^{-1}$)
J_0	initial permeate flux ($m \cdot s^{-1}$)
J_{ST}	steady-state permeate flux ($m \cdot s^{-1}$)
K_B	complete blocking filtration constant ($m^{-2} \cdot s^{-1}$)
K_C	cake filtration constant ($m^{-4} \cdot s$)
K_I	intermediate blocking filtration constant (m^{-1})

K_S standard blocking filtration constant (m^{-3})
Re membrane tube flow Reynolds number (—)
r_C specific cake resistance per unit cake thickness (m^{-2})
R_M membrane resistance (m^{-1})
R_{PA} resistance due to adsorption onto pore (m^{-1})
R_{PB} resistance due to pore blocking (m^{-1})
R_{FD} fouling deposit resistance (m^{-1})
R_{BL} boundary layer resistance (m^{-1})
t time (s)
V permeate volume (m^3)

Greek Symbols

ΔP transmembrane pressure difference (Pa)
γ shear rate (s^{-1})
μ permeate viscosity (Pa·s)

REFERENCES

1. M. C. Porter, "Latex Concentration/Recovery," in *Handbook of Industrial Membrane Technology*, Noyes Publications, New Jersey, 1990, p. 229.
2. R. H. Davis, "Theory for Cross-Flow Microfiltration," in *Membrane Handbook* (W. S. Ho and K. K. Sirkar, Eds.), Van Nostrand Reinhold, New York, 1992, p. 483.
3. M. C. Porter, "Concentration Polarization with Membrane Ultrafiltration," *Ind. Eng. Chem., Prod. Res. Dev., 11*, 233 (1972).
4. M. H. Lojkine, R. W. Field, and J. A. Howell, "Cross-Flow Microfiltration of Cell Suspensions: A Review of Models with Emphasis on Particle Size Effects," *Trans. Inst. Chem. Eng., Part C, 70*, 149 (1992).
5. A. L. Zydney and C. K. Colton, "A Concentration Polarization Model for the Filtrate Flux in Cross-Flow Microfiltration of Particulate Suspensions," *Chem. Eng. Commun., 47*, 1 (1986).
6. G. Green and G. Belfort, "Fouling of Ultrafiltration Membranes: Lateral Migration and the Particle Trajectory Model," *Desalination, 35*, 129 (1980).
7. D. A. Drew, J. A. Schonberg, and G. Belfort, "Lateral Inertial Migration of a Small Sphere in Fast Laminar Flow through a Membrane Duct," *Chem. Eng. Sci., 46*, 3219 (1991).
8. R. M. McDonogh, A. G. Fane, and C. J. D. Fell, "Charge Effects in the Cross-Flow Filtration of Colloids and Particulates," *J. Membr. Sci., 43*, 69 (1989).
9. P. Mikulášek and P. Doleček, "Characterization of Ceramic Tubular Membranes by Active Pore Size Distribution," *Sep. Sci. Technol., 29*, 1183 (1994).
10. P. C. Carman, *Flow of Gases through Porous Media*, Butterworths, London, 1956.
11. P. H. Hermans and H. L. Bredée, "Zur kenntniss der filtrationsgesetze," *Rec. Trav. Chim., 54*, 680 (1935).
12. J. Hermia, "Constant Pressure Blocking Filtration Laws. Application to Power Law Non-Newtonian Fluids," *Trans. Inst. Chem. Eng., 60*, 183 (1982).
13. A. Rushton, M. Hosseini, and H. Rushton, "Shear Effects in Cake Formation Mechanisms," *Filtr. Separ., 22*, 58 (1985).

14. C. Visvanathan and R. Ben Aim, "Studies on Colloidal Membrane Fouling Mechanisms in Cross-Flow Microfiltration," *J. Membr. Sci.*, *45*, 3 (1989).
15. G. Gésan, G. Daufin, U. Merin, J. P. Labbé, and A. Quemerais, "Fouling during Constant Flux Cross-Flow Microfiltration of Pretreated Whey. Influence of Transmembrane Pressure Gradient," *Ibid.*, *80*, 131 (1993).
16. B. Reismeier, K. H. Kroner, and M. R. Kula, "Tangential Filtration of Microbial Suspensions: Filtration Resistance and Model Development," *J. Biotechnol.*, *12*, 153 (1989).
17. W. R. Bowen and X. Goenaga, "Properties of Microfiltration Membranes, Part 3, Effect of Physicochemical Conditions on Cross-Flow Microfiltration at Aluminium Oxide Membranes," *I. E. Chem. E. Symp. Ser.*, *118*, 81 (1990).
18. B. R. Midmore, D. Diggins, and R. J. Hunter, "The Effect of Temperature and Ion Type on the Effective Charge in Polystyrene Latices," *J. Colloid Interface Sci.*, *129*, 153 (1989).

Received by editor April 20, 1995